Highly efficient induction of functionally mature excitatory neurons from feeder-free human ES/iPS cells.

Zhi Zhou[a]*, Wataru Kakegawa[a], Koki Fujimori[a], Misato Sho[a], Rieko Shimamura[a], Supakul Sopak[a], Sho Yoshimatsu[a], Jun Kohyama[a], Michisuke Yuzaki[a] and Hideyuki Okano[a]*

[a] Department of Physiology, School of Medicine, Keio University, Tokyo, Japan

* Corresponding authors: Zhi Zhou and Hideyuki Okano, Department of Physiology, School of Medicine, Keio University, 35 Shinanomachi Shinjuku-ku, Tokyo, 160-8582, Japan

E-mail address: zhouzhi0124@gmail.com (Z.Z.), hidokano@a2.keio.jp (H.O.)

Abstract

Cortical excitatory neurons (Cx neurons) are the most dominant neuronal cell type in the cerebral cortex and play a central role in cognition, perception, intellectual behavior, and emotional processing. Robust *in vitro* induction of Cx neurons may facilitate as a tool for the elucidation of brain development and the pathomechanism of the intractable neurodevelopmental and neurodegenerative disorders, including Alzheimer's disease, and thus potentially contribute to drug development. Here, we report a defined method for the efficient induction of Cx neurons from the feeder-free-conditioned human embryonic stem cells (ES cells) and induced pluripotent stem cells (iPS cells). Using this method, human ES/iPS cells could be differentiated into ~99% MAP2-positive neurons by three weeks, and these induced neurons displayed several characteristics of mature excitatory neurons within 5 weeks, such as strong expression of glutamatergic neuron-specific markers (subunits of AMPA and NDMA receptors and CAMKIIα), highly synchronized spontaneous firing and excitatory postsynaptic current (EPSC). In addition, the Cx neurons showed susceptibility to $A\beta_{42}$ oligomer toxicity and excessive glutamate excitotoxicity, which is another advantage for toxicity testing and searching for therapeutic agent discovery. Taken together, this study provides a novel research platform for studying neural development and degeneration based on the feeder-free human ES/iPS cell system.

Keywords: cortical excitatory neuron, neuronal differentiation, induced pluripotent stem cell

Introduction

Cortical excitatory neurons (Cx neurons) represent approximately 80% of all neurons in the cerebral cortex, where they play a central role in cognition, perception, intellectual behavior, and emotional processing [1]. Using glutamate as their neurotransmitter, Cx neurons, also known as projection neurons, are integrated into higher-order neuronal networks, and their activity is locally modulated by inhibitory GABAergic neurons, which represent approximately 20% of the neuronal population within the cerebral cortex. Because of their important roles, the developmental abnormalities and the degeneration of Cx neurons could lead to a variety of intractable neurological disorders, such as autism spectrum disorder (ASD), frontotemporal dementia (FTD), and Alzheimer's disease (AD). Furthermore, previous studies have shown that the enrichment of neurons with a region-specific identity can recapitulate disease-associated phenotypes *in vitro* [2-4]. Thus, a robust *in vitro* induction of Cx neurons *in vitro* holds great promise for high-throughput screening of therapeutic candidates for these diseases.

Human embryonic stem cells (ES cells) and induced pluripotent stem cells (iPS cells) have the potential for unlimited proliferation and differentiation into all three germ layers [5,6]. Based on pioneering studies on neural differentiation of mouse and human ES/iPS cells [7,8], the induction of Cx neurons from human ES/iPS cells has been reported by various groups [2,9-16]. However, there are several technical and biological limitations to these methods. For example, first, the reported methods used on-feeder human ES/iPS cells as the starting material, in which the maintenance of on-feeder human ES/iPS cells requires heterogenous feeder cells such as primary mouse embryonic fibroblasts (MEFs) or STO feeder cells [17]. The preparation of feeder cells, including a large-scale expansion and a mitotic inactivation, requires considerable effort. In addition, due to the difficulty of completely eliminating feeder cells, residual feeders may hinder the successful differentiation of directed linage. Second, several reported methods have sued a 3D culture system. Direct floating culture of ES/iPS cells, so-called embryoid bodies (EB) [18,19], neurosphere [2] or organoids [14,15], usually results in a population of differentiated cells with developmental heterogeneity (neural stem cells located in the center, and neurons in the edge). Furthermore, cell-autonomous formation of anterior-posterior and dorsal-ventral axes is often observed in floating cell aggregates during 3D culture. Importantly, these 3D methods require a long-term differentiation culture (over 2~3 months) in order to obtain functional mature neurons, which may be costly and not favorable for high-throughput screening.

To circumvent these limitations, we report here a defined method for the direct differentiation of Cx

neurons from feeder-free human ES/iPS cells. By step-by-step optimization of the differentiation procedures, we demonstrated a successful induction of Cx neurons with high efficiency (~ 100%).

Material and Methods

Ethical statements

Human ES/iPS experiments cells were approved by the Ministry of Education, Culture, Sports, Science, and Technology (MEXT) of Japan and the Ethics Committee of Keio University School of Medicine (approval number: 20080016). Recombinant DNA experiments were approved by the Safety Committee for Recombinant DNA Experiments of Keio University.

Cell culture

In the present study, we used two human iPS cell lines (201B7 and 1210B2) and one human ES cell line (KhES1) in the present study, which were kindly provided by Drs. Shinya Yamanaka and Norio Nakatsuji (Kyoto University) [6,20,21]. We also used a disease-specific iPS cell line PS1 (A246E), which was established from a patient with familial Alzheimer's disease patient with an Ala246Glu mutation in *Presenilin 1* [22]. These ES/iPS cells were maintained in a feeder-free condition as described previously [20,23,24]. Briefly, the ES/iPS cells were maintained in StemFit/AK02N (Wako (Ajinomoto), AJ100). We used 0.5× TrypLE select (Thermo Fisher Scientific) in PBS(-) for passaging and single-cell dissociation and plated them on a 6-well tissue culture plate with the AK02N medium supplemented with 10 µM Y27632 (Wako, 253-00513) for initial 24 h. The culture plates were pre-coated with 1.5 µg/ml iMatrix-511 silk (Laminin-511 E8; Wako (Nippi), 381-07363). Medium change was changed every other day, and passaging was performed every 7-10 d.

Neuronal differentiation

For neuronal differentiation, single-cell-dissociated human ES/iPS cells were plated on a Laminin-511 E8-coated tissue culture plate (4.17×10^4 cells/cm^2, 4.0×10^5/well for 6-well plates, 1.62×10^5/well for 12-well plates, 7.83×10^4/well for 24-well plates, 3.1×10^4/well for 48-well plates) in the AK02N medium supplemented with 10 µM Y27632 (Y27632 was added only for the first 24 h). After plating, the ES/iPS cells were initially maintained in AK02N medium until the cell density reached sub-confluent (80 – 90%). The medium was then changed to a GMEM/KSR medium supplemented with 2 µM DMH1 (Wako, 041-33881), 2 µM SB431542 (Sigma, S4317) and 10 µM Y27632 (defined as 0 day(s) *in vitro*; 0 div). The GMEM/KSR medium consisted of 1 × Glasgow's MEM (GMEM; Wako, 078-05525) supplemented with 8% KnockOut Serum Replacement (KSR; Thermo Fisher

Scientific, 10828-028). In the initial optimization experiments, we also used MHM/B27 [2] and N2/B27 media [25]. From 1 to 14 div, the medium was changed daily using the same medium, except that Y27632 was removed from 1 div, and DMH1 and SB431542 were removed at 8 div. At 15 div, cells were washed once in PBS and then incubated with 1 × Accutase (Nacalai Tesque, 12679-54) for 30 m at 37°C for single-cell dissociation. The dissociated cells were initially collected in GMEM/8%KSR containing 10 μM Y27632. After centrifugation (200 × g, 5 m) and removal of the supernatant, the cells were resuspended in a plating medium. The plating medium consisted of 1 × BrainPhys Neuronal Medium/N2-A/SM1 kit (BrainPhys; Stem Cell Technologies, 05793) supplemented with 10 μM Y27632, 10 ng/ml BDNF (R&D Systems, 248-BD-025), 10 ng/ml GDNF (Peprotech, 450-10), 200 μM ascorbic acid (AA; Sigma, A4403-100MG), 0.5 mM dbcAMP (Sigma, D0627-1G), 10 μM DAPT (Sigma, D5942-5MG), and 2 μM PD0332991 (Sigma, PZ0199). Prior to plating, the cell suspension was filtrated through a 40-μm cell strainer to remove aggregated cells. Cells were plated onto a Poly-L-Lysine and Laminin-coated 24-well plate at a density of 4.0 x 10^5 cells/well. Poly-L-Lysine and Laminin coating of 24-well plates was performed by incubation for 48 h at 37°C with Tissue Culture water (Sigma, W3500) supplemented with 1 μg/ml poly-L-Lysine (Sigma, P4832) and 4 ng/ml mouse Laminin (Thermo Fisher Scientific, 23017015). At day 18, half of the medium was changed to a maintenance medium containing 10 μM DAPT. The maintenance medium consisted of 1 × BrainPhys supplemented with 10 ng/ml BDNF, 10 ng/ml GDNF, 200 μM ascorbic acid, 0.5 mM dbcAMP and 2 μM PD0332991. At 21 div, a complete medium change was performed using the maintenance medium. After 24 div, the medium was changed every 3 d with the same medium.

qRT-PCR

RNA extraction, reverse transcription, and qRT-PCR were performed as previously described [26]. The level of *ACTB* expression was used as an internal control for normalization. Total cDNA from an adult human sample was used as a control for the cerebral cortex.

Immunocytochemistry

Immunocytochemistry was performed as previously described [26]. For high-content quantitative immunocytochemical analysis, we used the IN Cell Analyzer 6000 (GE Healthcare) as described previously [3]. The detailed analysis protocol using IN Cell Analyzer 6000 is available upon request. Information on the primary and secondary antibodies used in this study is available from the corresponding authors.

ELISA

Enzyme-linked immunosorbent assay (ELISA) was performed as previously described [27]. Briefly, we collected culture media from Cx neurons. The collected media were briefly centrifuged to insoluble material and can be stored at -80℃ until the analysis. The remaining cells were lysed in RIPA buffer (Wako), and protein concentration was measured by BCA Protein assay (Pierce). A β 40 and Aβ42 levels in the media were measured using commercial kits, Human βAmyloid (1–40) Kit II (Wako, 298–64601) and Human βAmyloid (1–42) ELISA Kit High Sensitive (Wako, 296–64401) according to the manufacturer's instructions. Each Aβ concentration was normalized to the protein level of the culture cells.

Electrophysiology and Ca imaging

Microelectrode array (MEA) recording was performed using the Maestro system (Axion as previously described [28]. Briefly, 12-well MEA plates were pre-coated with poly-L-Lysine and Laminin, and neural progenitors (at 15 div) were subsequently plated onto the electrode surface in MEA plate. Data were acquired at a sampling rate of 12.5 kHz and filtered with a 200–3000 Hz Butterworth bandpass filter. The detection threshold was set to +6.0 × SD of the baseline electrode noise. Spike raster plots were analyzed using the Neural Metric Tool (Axion Biosystems). The spike count files generated from the recordings were used to calculate the number of active electrodes (defined as an electrode with an average of more than 5 spikes/min) in each well, the average mean firing rate (MFR or spikes/min) per active electrode, and the standard deviation of the average MFR per active electrode. The first 3 minutes of data in each data file were omitted to allow activity to stabilize in the Maestro, and 10–15 min of activity was subsequently recorded.

Calcium (Ca) imaging was performed as previously described [23]. Briefly, Fluo-8 (AAT Bioquest; final 5 μM), Probenecid (final 1 mM), Pluonic F-127 (final 0.02%) and Hoechst (final 0.5 μg/ml) were added to the plating medium and incubated for 30 min at 37℃. After incubation, the cells were washed twice with PBS and supplied with a fresh medium. For TTX or CNQX treatment, the reagent was supplemented to a final concentration of 2 μM or 50 μM, respectively. Movies were captured using an IX83 inverted microscope (Olympus) equipped with an electron-multiplying CCD camera (Hamamatsu Photonics) and a pE-4000 LED illumination system (CoolLED). We recorded the Ca oscillation of the cells using the MetaMorph Image Analysis Software with the following parameters: 12 outputs, 750 msec interval for 2 min, GFP filter, 1x gain, 2.75 MHz, and 80 msec exposure. Regions of interest (ROIs) were drawn on cells based on time projection images of the

recordings. ROI traces of the time course of changes in green fluorescence intensity were generated and used as substrates for subsequent analyses. To adjust for photobleaching, the difference in intensity between the first and the last image was subtracted. The change in fluorescence intensity over time was normalized as $\Delta F/F= (F-F0)/F0$, where F0 is the fluorescence at the beginning of the exposure (time 0). ΔFmax was defined as the difference of the maximum change in $\Delta F/F$. Whole-cell patch clumping was performed as previously described [26].

Statistical Analysis

All data were expressed as mean ± SD. The statistical significance of differences was analyzed by the Welch's *t*-test. Differences of $P < 0.05$ were expressed as *, $P < 0.01$ as **, and $P < 0.001$ as ***, which were considered statistically significant.

Results

Efficient induction of neural progenitors with a cerebrocortical identity from feeder-free human iPS cells

First, we sought to develop an optimized method to induce SOX1(+) incipient ectodermal cells from 201B7 healthy-control human iPS cells [6] cultured in a feeder-free condition using AK02N as the culture medium and iMatrix-511 as the coating material [20,24]. Based on the principle methodology described in previous studies [2,9-13,29,30], we tested a 7-day culture of iPS cells using three media, such as N2B27 [25], MHM/B27 [2] and GMEM/KSR [31] without supplementation of any chemical compounds (see Materials and Methods). FACS analysis using cell-permeable antibodies revealed that, among the culture media, GMEM/KSR medium resulted in the highest yield of SOX1(+) cells compared to those of N2B27 and MHM/B27 media (Supplementary Figure 1A).

Next, we performed simultaneous quantification of SOX1(+) cells and OCT4(+) pluripotent cells, as the remaining pluripotent cells may interfere with the subsequent neuronal differentiation due to their high proliferation rate and unpredictable differentiation into other lineages. In addition, we tested the addition of a BMP4 inhibitor, DMH1, and a TGF-β inhibitor, SB431542, to prevent the cells from the non-ectodermal differentiation [7]. When using the N2B27 medium, although DMH1 and SB431542 treatment improved the SOX1(+)/OCT4(-) rates, we observed approximately 30–60% remaining OCT4(+) cells (Supplementary Figure 1B). On the other hand, when using the GMEM/KSR medium, we found higher rates of SOX1(+)/OCT4(-) cells and very low rates of

OCT4(+) cells (~ 5%) in combination with DMH1 and SB431542 treatment (Supplementary Figure 1C). Therefore, we decided to focus on the method using the GMEM/KSR medium supplemented with DMH1 and SB431542 during the initial phase of induction (Left part of Figure 1A) for further analyses. Using total RNA derived from the differentiated cells at 12 div (days *in vitro*) and the undifferentiated iPS cells, we compared the gene expressions of pluripotency (*NANOG* and *POU5F1*), neuroectoderm (*SOX1* and *PAX6*) and cerebral cortex (*FOXG1* and *SIX*3)-related marker genes (Figure 1B). As a result, the differentiated cells showed significant upregulation of *SOX1*, *PAX6*, *FOXG1*, and *SIX3*, and downregulation of *NANOG* and *POU5F1* compared to the iPS cells (Figure 1B). Since low-dose treatment (2 μM each) of DMH1 and SB431542 showed a marginal increase in *SOX1* expression compared to that of high-dose treatment (5 and 10 μM) (data not shown), subsequent experiments were performed in the low-dose condition. In this condition, we also evaluated the time-dependent change of the marker gene expression by qRT-PCR (Supplementary Figure 2A) and immunocytochemistry (Supplementary Figure 2B). Taken together, these data demonstrate that our optimized method allows robust induction of neural progenitors with the cerebral cortex identity.

Maturation culture of neural progenitors with a CDK inhibitor

Using single-cell dissociation and subsequent replating of neural progenitors at 15 div, we next attempted to further differentiate these cells into functional mature neurons (right part of Figure 1A). Based on our preliminary results that the BrainPhys-based medium, but not the Neurobasal-based medium, enhanced neuronal survival and spontaneous firing activity of the differentiated cells as assessed by Ca imaging (data not shown), we used the BrainPhys medium supplemented with GDNF, BDNF, ascorbic acid (AA) and dbcAMP for neuronal survival and maturation. We also supplemented a γ-secretase inhibitor DAPT and the CDK4/6 inhibitor PD0332991 to further neuronal differentiation by promoting cell cycle exit [16]. Because prolonged γ-secretase inhibition may impair neuronal function [32], DAPT was discontinued on day 21. To facilitate further analyses, we first compared three coating conditions before replating neuronal progenitors as follows: poly-L-Lysine/Laminin, Matrigel, and Laminin only. Six days after replating, we found the lowest number of cell aggregations in the poly-L-Lysine/Laminin condition (Supplementary Figure 3A). Using the optimized BrainPhys medium and coating conditions, we observed a time-dependent increase in *SYN1*, *DLG4* (*PSD-95*) and *CAMK2A* gene expression upon 5–6 or 7–8 weeks after iPS cell differentiation (Figure 1C). We also confirmed the increase of glutamate ionotropic receptor genes essential for the functional maturation of glutamatergic neurons (Supplementary Figure 3B),

and the Alzheimer's disease-associated marker Tau (*MAPT*) and its postnatal-specific 4R isoform (Supplementary Figure 3C). In addition, the immunocytochemical analysis revealed that most of the differentiated cells (5 weeks after differentiation) were positive for MAP2, Foxg1, and NeuN (Figure 1D). In view of these results, the cells differentiated for 5 weeks or more are hereafter referred to as Cx neurons. In addition, we found that the Cx neurons (10 weeks after differentiation) showed punctate immunoreactivity of synaptic markers including SynI, vGluT1, vGluT2, and Homer1, indicating the formation of functional synapses (Figure 1E).

Electrophysiological analyses of the Cx neurons

To determine the formation of functional synapses and local circuits, we performed Calcium (Ca) imaging analysis of the Cx neurons using the fluorescent Ca indicator Fluo-8 (Materials and Methods). We recorded Ca dynamics at 15+7, 15+21, 15+36 and 15+94 div (Video S1–4). While differentiated cells on 15+7 and 15+21 div showed only spontaneous firing-like Ca flux (Video S1–2), Cx neurons on 15+36 and 15+94 div showed synchronized firing-like Ca flux (Video S3–4). Furthermore, using the Cx neurons at 15+36 div, we demonstrated that the treatment with the sodium channel blocker TTX completely abolished spontaneous firing-like Ca flux (data not shown), and the treatment with an AMPA/kainate receptor antagonist CNXQ failed to synchronize Ca flux (Figure 2A), suggesting that these synchronized Ca dynamics may be caused by functional synaptic activity.

To directly assess the electrophysiological properties of the Cx neurons, we also performed a whole-cell patch clamp and microelectrode array (MEA) analysis (Figure 2B–C and Supplementary Figure 4). The whole-cell patch clump revealed the spontaneous action potential (sAP) of Cx neurons (15+34 div; 10 out of 16 cells) (Figure 2B, top) and the excitatory postsynaptic current (sEPSC) (Figure 2C). The sAP was subsequently abolished after the TTX treatment (Figure 2B, bottom). By MEA analysis, we detected synchronized spontaneous firing of the Cx neurons at 15+35 div (Supplementary Figure 4). Taken together, we demonstrated that the Cx neurons were functionally mature and capable of forming local neuronal circuits through the excitatory synapses.

Susceptibility to toxic agents

To explore the glutamatergic neuron-specific susceptibility of the Cx neurons to the known neurotoxic agents, we first tested the supplementation of excessive L-glutamate (L-Glu), which induces cell death by excessive excitotoxicity through glutamate receptors [33]. As shown in Figure 3A, we performed high-content imaging analysis of the Cx neurons using the IN CELL Analyzer. L-Glu toxicity was evaluated by MAP2(+) neurite length and WST-8 bioreduction-based cell

viability assay. As a result, supplementation of excessive glutamate, 12.5 μM or more, caused a decrease in neurite length per cell (Figure 3A–B) and WST-8 bioreduction activity (Figure 3C). On the other hand, supplementation with an NMDA glutamate receptor antagonist MK801 (1 μM) partially attenuated the toxicity of excessive L-Glu (Figure 3A–C), suggesting that the effect was mediated by glutamate receptors expressed in the Cx neurons.

We next investigated the applicability of the Cx neurons for *in vitro* modeling of Alzheimer's disease. Supplementation of Aβ42 oligomer in the Cx neuron culture (Figure 4A) resulted in a dose-dependent decrease in neurite length per cell (Figure 4B) and WST-8 bioreduction activity (Figure 4C). We also examined the endogenous secretion of Aβ40 and Aβ42 from the Cx neurons. Supplementation with DAPT dramatically decreased the secretion of Aβ40 (Figure 4D). Using the Cx neurons differentiated from a familial Alzheimer's patient-derived iPS cell line, PS1 (A246E) [22], we found that disease-specific phenotypes such as decreased Aβ40 secretion (Figure 4E, left), increased Aβ42 secretion (Figure 4E, middle) and thus increased ratio of Aβ42/Aβ40 ratio (Figure 4E, right) were recapitulated. Thus, we demonstrated that the use of the Cx neurons was advantageous for recapitulating region-specific neurological pathology.

Reproducibility of the induction method in multiple human ES/iPS cell lines

Finally, we evaluated the reproducibility of the induction method using other human ES/iPS cell lines of different origins, such as 1210B2 and KhES1 (Supplementary Figure 5A). We showed that these two lines were successfully differentiated into MAP2-positive neurons with high efficiencies comparable to that of 201B7 (data not shown). Furthermore, we demonstrated by electrophysiology analysis that Cx neurons derived from these lines exhibited a maturity that was susceptible to the toxicity test of L-Glu (Supplementary Figure 5B) and Aβ42 oligomer (Supplementary Figure 5C).

Discussion

In the present study, we report a defined method for the induction of Cx neurons from the feeder-free human ES/iPS cells. We highlight three advantages of this method as follows: (i) High efficiency of neuronal induction with a region (cerebral cortex)-specific identity, which is important for recapitulation of disease-specific phenotypes [2-4]. (ii) High reproducibility across multiple cell lines, which is essential for unbiased comparison and robust applicability to disease-specific lines. In particular, since much of the underlying genetic/epigenetic mechanisms of sporadic diseases remain unclear, we believe that *in vitro* systems with high purity and reproducibility could address this issue.

(iii) Simplicity of the method. Our initial motivation was to explore the ease of use for high-throughput screening using human ES/iPS cells. To this end, we took advantage of feeder-free human ES/iPS cells, and also succeeded in shortening the induction period required to obtain functional mature neurons (to 5 weeks). This allows for cost-effective screening of therapeutic candidates using Cx neurons.

Amyloid beta, including Aβ40 and Aβ42, is the major component of senile plaques found in the brains of Alzheimer's disease patients. Whether and how amyloid beta causes neurodegeneration in patients' brains is still unclear and under debate, our data suggested that Cx neurons induced by our method could be directly applicable for elucidating this mechanism *in vitro*, as the endogenous Aβ secretion activity was enough for recapitulating the mutant Presenilin 1-associated Alzheimer's disease phenotype (Figure 4D–E). However, while the addition of DAPT, the γ-secretase inhibitor, could potentially alter the results of the Aβ analysis, our additional induction of other cell lines indicated the importance of adding DAPT to obtain high-quality Cx neurons as the cells showed higher survival rates with the addition of DAPT (paper in preparation).

Furthermore, the functional maturation of the Cx neurons, as shown by our data in electrophysiological analysis (Figure 2 and Supplementary Figures 4 and 5C), *CAMK2A* and 4R-Tau expression (Figure 1C and Supplementary Figure 3D), also indicated that the induced Cx neurons are also applicable for recapitulating the late-onset disease phenotypes. Although further analysis is required, we have demonstrated that the method reported here may serve as a novel research platform for unraveling cerebral cortex-specific pathomechanisms of neurological disorders and thus may also contribute to drug screening and development.

Acknowledgment

We especially thank Drs. Hirotaka Watanabe and Mitsuru Ishikawa (Keio University) for helpful discussion, and all the laboratory members of H.O. and M.Y. for encouragement and generous support for this study. This study was funded by the MEXT and the AMED (Grant ID: JP20dm0207001 to H.O.).

References

[1] J.L. Rubenstein, Annual Research Review: Development of the cerebral cortex: implications for neurodevelopmental disorders, J Child Psychol Psychiatry, 52 (2011) 339-355.

[2] K. Imaizumi, T. Sone, K. Ibata, K. Fujimori, M. Yuzaki, W. Akamatsu, H. Okano, Controlling the Regional Identity of hPSC-Derived Neurons to Uncover Neuronal Subtype Specificity of Neurological

Disease Phenotypes, Stem Cell Reports, 5 (2015) 1010-1022.

[3] K. Fujimori, M. Ishikawa, A. Otomo, N. Atsuta, R. Nakamura, T. Akiyama, S. Hadano, M. Aoki, H. Saya, G. Sobue, H. Okano, Modeling sporadic ALS in iPSC-derived motor neurons identifies a potential therapeutic agent, Nat Med, 24 (2018) 1579-1589.

[4] S.Y. Ng, B.S. Soh, N. Rodriguez-Muela, D.G. Hendrickson, F. Price, J.L. Rinn, L.L. Rubin, Genome-wide RNA-Seq of Human Motor Neurons Implicates Selective ER Stress Activation in Spinal Muscular Atrophy, Cell Stem Cell, 17 (2015) 569-584.

[5] J.A. Thomson, J. Itskovitz-Eldor, S.S. Shapiro, M.A. Waknitz, J.J. Swiergiel, V.S. Marshall, J.M. Jones, Embryonic stem cell lines derived from human blastocysts, Science, 282 (1998) 1145-1147.

[6] K. Takahashi, K. Tanabe, M. Ohnuki, M. Narita, T. Ichisaka, K. Tomoda, S. Yamanaka, Induction of pluripotent stem cells from adult human fibroblasts by defined factors, Cell, 131 (2007) 861-872.

[7] S.M. Chambers, C.A. Fasano, E.P. Papapetrou, M. Tomishima, M. Sadelain, L. Studer, Highly efficient neural conversion of human ES and iPS cells by dual inhibition of SMAD signaling, Nat Biotechnol, 27 (2009) 275-280.

[8] K. Watanabe, D. Kamiya, A. Nishiyama, T. Katayama, S. Nozaki, H. Kawasaki, Y. Watanabe, K. Mizuseki, Y. Sasai, Directed differentiation of telencephalic precursors from embryonic stem cells, Nat Neurosci, 8 (2005) 288-296.

[9] N. Gaspard, T. Bouschet, A. Herpoel, G. Naeije, J. van den Ameele, P. Vanderhaeghen, Generation of cortical neurons from mouse embryonic stem cells, Nat Protoc, 4 (2009) 1454-1463.

[10] I. Espuny-Camacho, K.A. Michelsen, D. Gall, D. Linaro, A. Hasche, J. Bonnefont, C. Bali, D. Orduz, A. Bilheu, A. Herpoel, N. Lambert, N. Gaspard, S. Peron, S.N. Schiffmann, M. Giugliano, A. Gaillard, P. Vanderhaeghen, Pyramidal neurons derived from human pluripotent stem cells integrate efficiently into mouse brain circuits in vivo, Neuron, 77 (2013) 440-456.

[11] Y. Shi, P. Kirwan, F.J. Livesey, Directed differentiation of human pluripotent stem cells to cerebral cortex neurons and neural networks, Nat Protoc, 7 (2012) 1836-1846.

[12] P. Kirwan, B. Turner-Bridger, M. Peter, A. Momoh, D. Arambepola, H.P. Robinson, F.J. Livesey, Development and function of human cerebral cortex neural networks from pluripotent stem cells in vitro, Development, 142 (2015) 3178-3187.

[13] S.P. Pasca, T. Portmann, I. Voineagu, M. Yazawa, A. Shcheglovitov, A.M. Pasca, B. Cord, T.D. Palmer, S. Chikahisa, S. Nishino, J.A. Bernstein, J. Hallmayer, D.H. Geschwind, R.E. Dolmetsch, Using iPSC-derived neurons to uncover cellular phenotypes associated with Timothy syndrome, Nat Med, 17 (2011) 1657-1662.

[14] T. Kadoshima, H. Sakaguchi, T. Nakano, M. Soen, S. Ando, M. Eiraku, Y. Sasai, Self-organization of

axial polarity, inside-out layer pattern, and species-specific progenitor dynamics in human ES cell-derived neocortex, Proc Natl Acad Sci U S A, 110 (2013) 20284-20289.

[15] M.A. Lancaster, M. Renner, C.A. Martin, D. Wenzel, L.S. Bicknell, M.E. Hurles, T. Homfray, J.M. Penninger, A.P. Jackson, J.A. Knoblich, Cerebral organoids model human brain development and microcephaly, Nature, 501 (2013) 373-379.

[16] V. Telezhkin, C. Schnell, P. Yarova, S. Yung, E. Cope, A. Hughes, B.A. Thompson, P. Sanders, C. Geater, J.M. Hancock, S. Joy, L. Badder, N. Connor-Robson, A. Comella, M. Straccia, G. Bombau, J.T. Brown, J.M. Canals, A.D. Randall, N.D. Allen, P.J. Kemp, Forced cell cycle exit and modulation of GABAA, CREB, and GSK3beta signaling promote functional maturation of induced pluripotent stem cell-derived neurons, Am J Physiol Cell Physiol, 310 (2016) C520-541.

[17] J.H. Park, S.J. Kim, E.J. Oh, S.Y. Moon, S.I. Roh, C.G. Kim, H.S. Yoon, Establishment and maintenance of human embryonic stem cells on STO, a permanently growing cell line, Biol Reprod, 69 (2003) 2007-2014.

[18] J.R. Smith, L. Vallier, G. Lupo, M. Alexander, W.A. Harris, R.A. Pedersen, Inhibition of Activin/Nodal signaling promotes specification of human embryonic stem cells into neuroectoderm, Dev Biol, 313 (2008) 107-117.

[19] Y. Okada, A. Matsumoto, T. Shimazaki, R. Enoki, A. Koizumi, S. Ishii, Y. Itoyama, G. Sobue, H. Okano, Spatiotemporal recapitulation of central nervous system development by murine embryonic stem cell-derived neural stem/progenitor cells, Stem Cells, 26 (2008) 3086-3098.

[20] M. Nakagawa, Y. Taniguchi, S. Senda, N. Takizawa, T. Ichisaka, K. Asano, A. Morizane, D. Doi, J. Takahashi, M. Nishizawa, Y. Yoshida, T. Toyoda, K. Osafune, K. Sekiguchi, S. Yamanaka, A novel efficient feeder-free culture system for the derivation of human induced pluripotent stem cells, Sci Rep, 4 (2014) 3594.

[21] N. Nakatsuji, Establishment and manipulation of monkey and human embryonic stem cell lines for biomedical research, Ernst Schering Res Found Workshop, (2005) 15-26.

[22] T. Yagi, D. Ito, Y. Okada, W. Akamatsu, Y. Nihei, T. Yoshizaki, S. Yamanaka, H. Okano, N. Suzuki, Modeling familial Alzheimer's disease with induced pluripotent stem cells, Hum Mol Genet, 20 (2011) 4530-4539.

[23] M. Ishikawa, T. Aoyama, S. Shibata, T. Sone, H. Miyoshi, H. Watanabe, M. Nakamura, S. Morota, H. Uchino, A.S. Yoo, H. Okano, miRNA-Based Rapid Differentiation of Purified Neurons from hPSCs Advancestowards Quick Screening for Neuronal Disease Phenotypes In Vitro, Cells, 9 (2020).

[24] T. Miyazaki, T. Isobe, N. Nakatsuji, H. Suemori, Efficient Adhesion Culture of Human Pluripotent Stem Cells Using Laminin Fragments in an Uncoated Manner, Sci Rep, 7 (2017) 41165.

[25] J. Lu, X. Zhong, H. Liu, L. Hao, C.T. Huang, M.A. Sherafat, J. Jones, M. Ayala, L. Li, S.C. Zhang, Generation of serotonin neurons from human pluripotent stem cells, Nat Biotechnol, 34 (2016) 89-94.

[26] Z. Zhou, K. Kohda, K. Ibata, J. Kohyama, W. Akamatsu, M. Yuzaki, H.J. Okano, E. Sasaki, H. Okano, Reprogramming non-human primate somatic cells into functional neuronal cells by defined factors, Mol Brain, 7 (2014) 24.

[27] M. Sho, N. Ichiyanagi, K. Imaizumi, M. Ishikawa, S. Morimoto, H. Watanabe, H. Okano, A combinational treatment of carotenoids decreases Abeta secretion in human neurons via beta-secretase inhibition, Neurosci Res, 158 (2020) 47-55.

[28] M. Isoda, J. Kohyama, A. Iwanami, T. Sanosaka, K. Sugai, R. Yamaguchi, T. Matsumoto, M. Nakamura, H. Okano, Robust production of human neural cells by establishing neuroepithelial-like stem cells from peripheral blood mononuclear cell-derived feeder-free iPSCs under xeno-free conditions, Neurosci Res, 110 (2016) 18-28.

[29] Y. Shi, P. Kirwan, J. Smith, H.P. Robinson, F.J. Livesey, Human cerebral cortex development from pluripotent stem cells to functional excitatory synapses, Nat Neurosci, 15 (2012) 477-486, S471.

[30] S.C. Zhang, M. Wernig, I.D. Duncan, O. Brustle, J.A. Thomson, In vitro differentiation of transplantable neural precursors from human embryonic stem cells, Nat Biotechnol, 19 (2001) 1129-1133.

[31] D. Doi, B. Samata, M. Katsukawa, T. Kikuchi, A. Morizane, Y. Ono, K. Sekiguchi, M. Nakagawa, M. Parmar, J. Takahashi, Isolation of human induced pluripotent stem cell-derived dopaminergic progenitors by cell sorting for successful transplantation, Stem Cell Reports, 2 (2014) 337-350.

[32] J. Shen, Function and dysfunction of presenilin, Neurodegener Dis, 13 (2014) 61-63.

[33] J. Lewerenz, P. Maher, Chronic Glutamate Toxicity in Neurodegenerative Diseases-What is the Evidence?, Front Neurosci, 9 (2015) 469.

Figure Legends

Figure 1. Optimization of the induction method.

(A) Graphical timeline of the induction method. For the detail, see the “Neuronal differentiation” section in Materials and Methods.

(B) qRT-PCR analysis of pluripotency (*NANOG* and *POU5F1*), neuroectoderm (*SOX1* and *PAX6*) and cerebral cortex (*FOXG1* and *SIX*3)-related markers in the original feeder-free-conditioned 201B7 iPS cells (DIV 0 Ff-iPS) and the differentiated cells at div 12 (DIV 12).

(C) qRT-PCR analysis of synaptic markers (*SYN1* and *DLG4*) and *CAMK2A*.

(D) Immunocytochemical analysis of the differentiated cells (5 weeks after differentiation). Nuclei were stained blue with Hoechst.

(E) Immunocytochemical analysis of the Cx neurons (10 weeks after differentiation).

Figure 2. Electrophysiological analysis.

(A) Ca imaging analysis using Fluo-8 in the Cx neurons at 15+36 div (Movie S3). Spikes were counted based on ΔF/F of the Fluo-8 fluorescence intensity. The vertical axis shows Neuron ID, and the horizontal axis shows time (sec). Synchronized spikes, found only in control cells, are shown as red lines.

(B–C) Whole-cell patch clump of the Cx neurons at 15+34 div.

Figure 3. Susceptibility of the Cx neurons to L-Glu.

(A) Representative immunocytochemical images of the Cx neurons with/without MK801 (1 μM) and L-Glu (50 μM) supplementation. Neurites were stained green with the MAP2 antibody.

(B–C) Dose-dependent toxicity of L-Glu (0, 12.5, 25, 50 and 100 μM) with/without MK801, analyzed by MAP2(+) neurite length (B) and WST-8 bioreduction activity (C). Absorbance at 460 nm of the Cx neurons (0 μM L-Glu, MK801(-) condition) is set to 100%.

Figure 4. Susceptibility of the Cx neurons to Aβ oligomer and endogenous Aβ secretion.

(A) Representative immunocytochemical images of the Cx neurons (201B7) with/without Aβ42 oligomer (0, 5, 10 μM). Neurites were stained green with the MAP2 antibody.

(B–C) Dose-dependent toxicity of Aβ42 oligomer (0, 1.25, 2.5, 5 and 10 μM), analyzed by MAP2(+) neurite length (B) and WST-8 bioreduction activity (C) Absorbance at 460 nm of the Cx neurons (0 μM Aβ42 oligomer condition) is set to 100%.

(D) ELISA of endogenous Aβ40 and Aβ42 secretion from the Cx neurons (differentiated from 201B7 and PS1 (A246E) iPS cells).

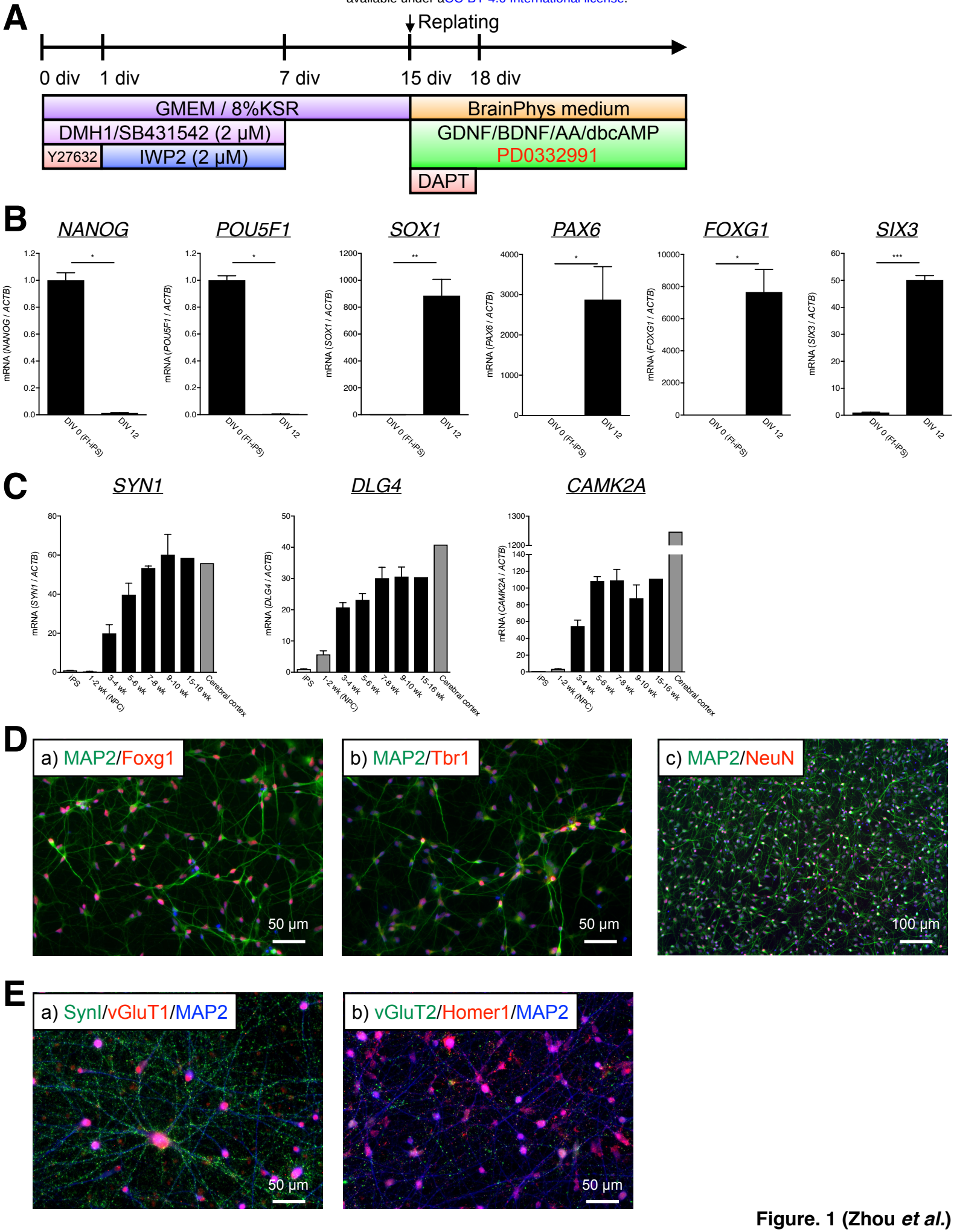

Figure. 1 (Zhou *et al.*)

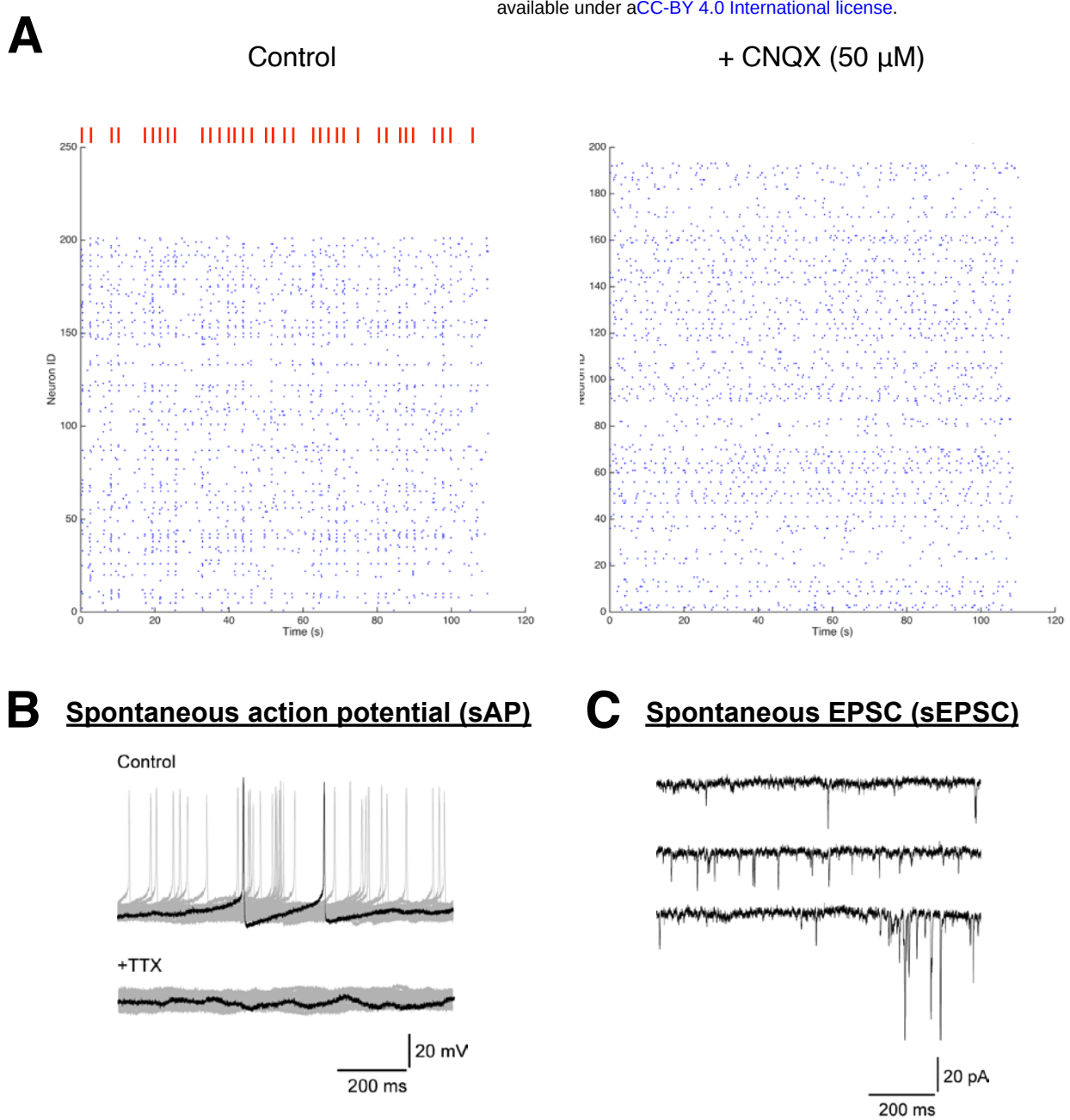

Figure. 2 (Zhou *et al.*)

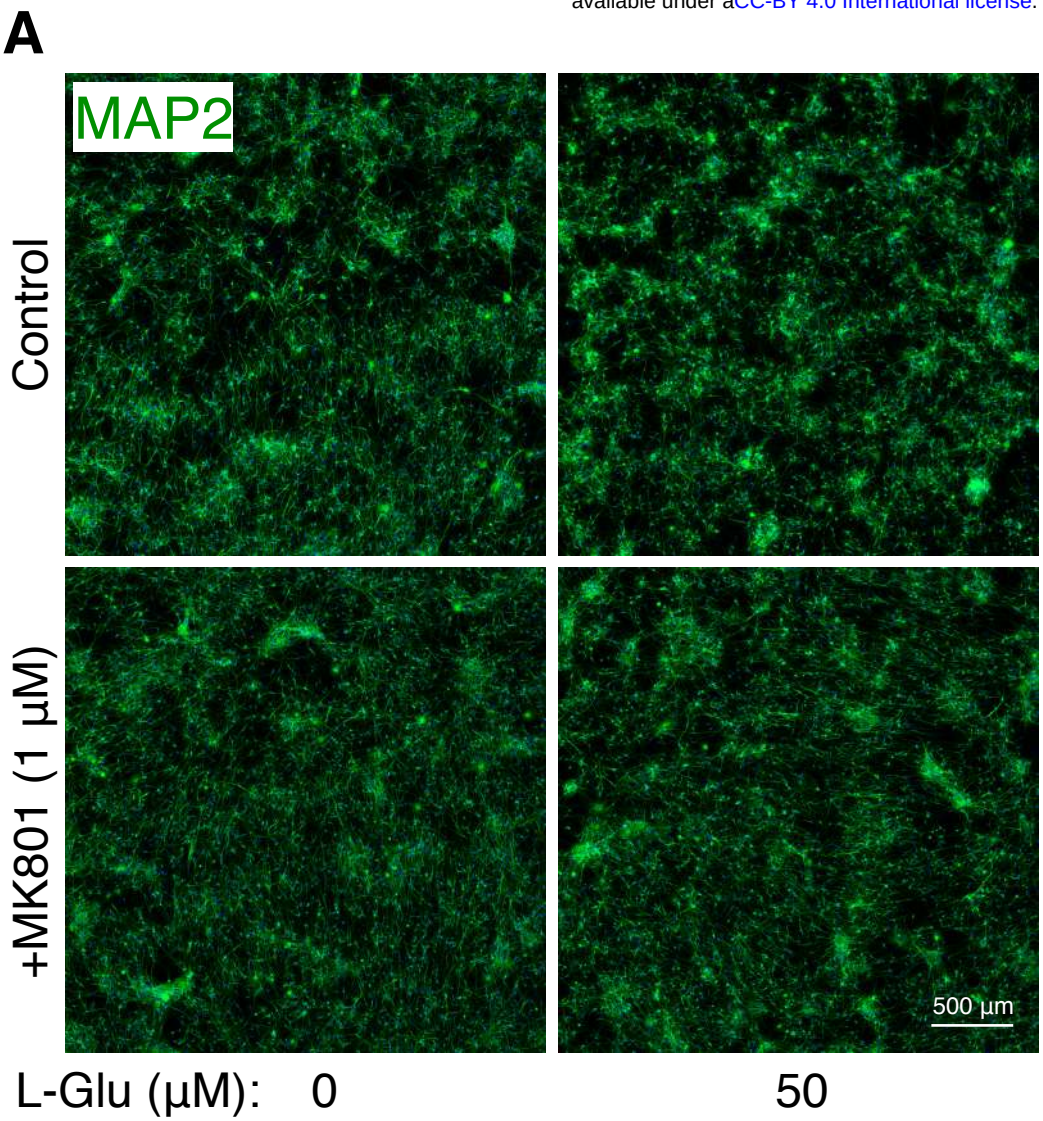

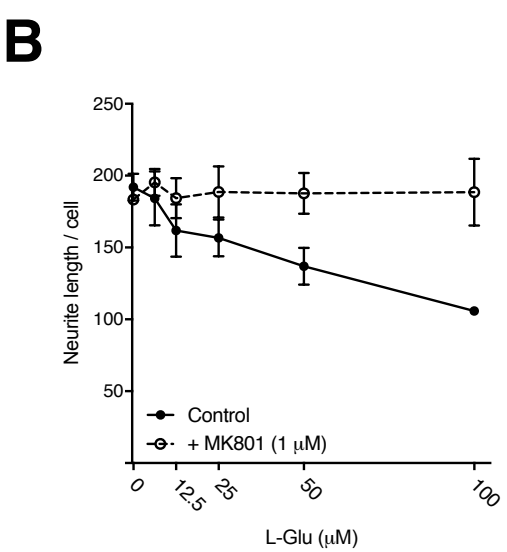

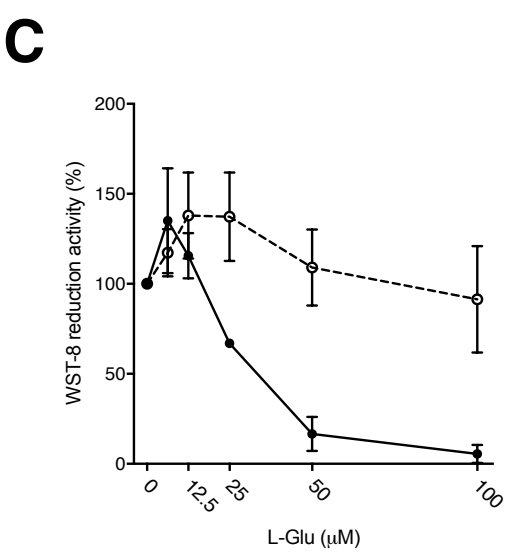

Figure. 3 (Zhou *et al.*)

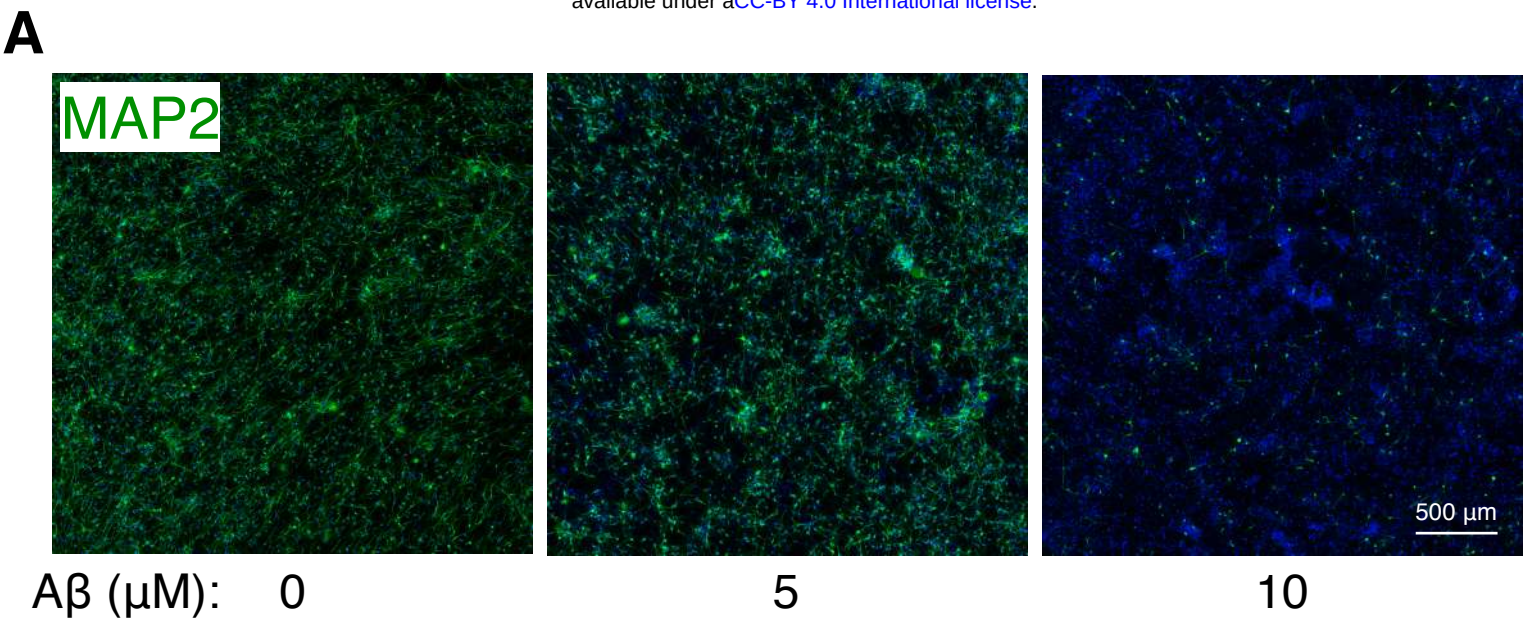

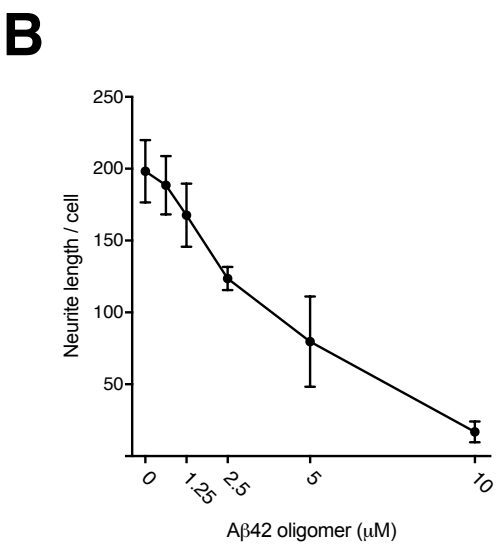

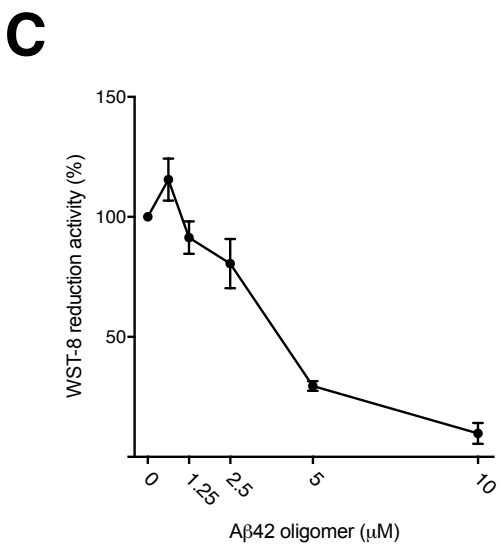

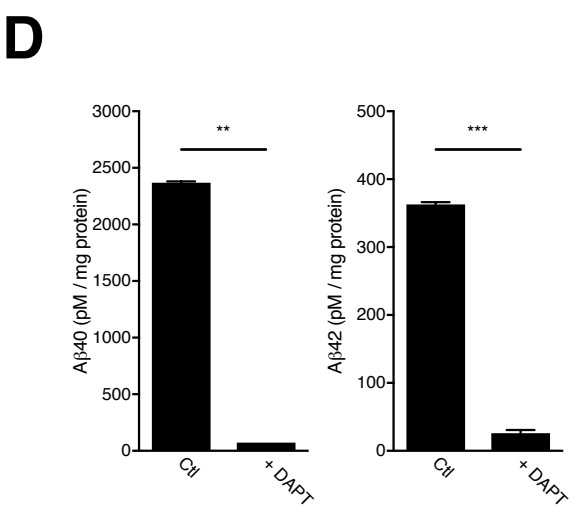

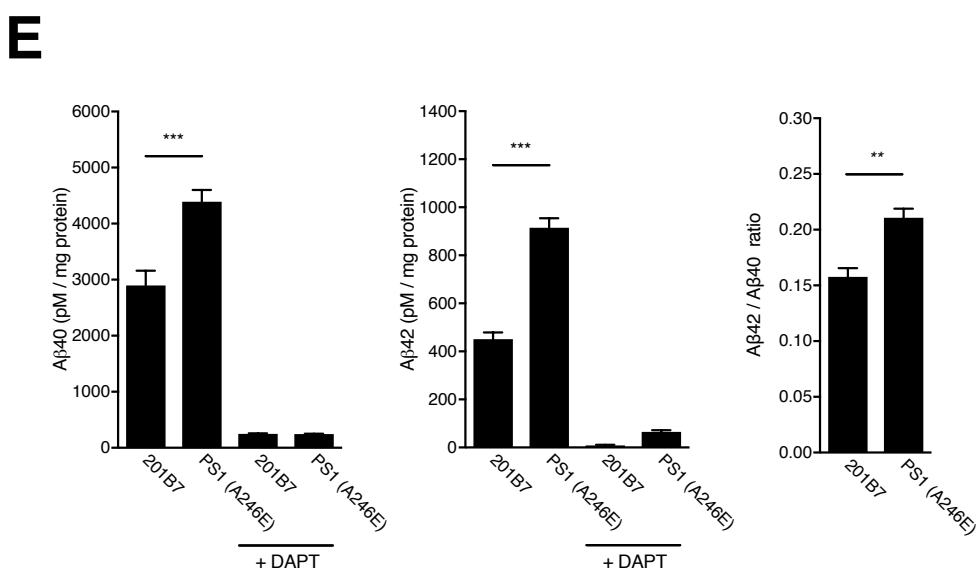

Figure. 4 (Zhou *et al.*)